The Nucleus **48**, No. 2 (2011) 91-99

The Nucleus
A Quarterly Scientific Journal of Pakistan
Atomic Energy Commission
NCLEAM, ISSN 0029-5698

THE IMPACT OF SINTERING PROMOTER OXIDES ON MAGNESIA-DOPED ZIRCONIA CRYSTALS SYNTHESIZED BY SOL SPRAY PYROLYSIS PROCESS

*S. K. DURRANI[1], S. REHMAN[2], F. QAZI[2], S.Z. HUSSAIN[1], M. AHMAD[3], M. ARIF[1] and B. MOHAMMAD[4]

[1] Materials Division, Directorate of Technology, PINSTECH, Nilore, Islamabad, Pakistan

[2] Institute of Chemical Sciences, University of Peshawar, Peshawar, Pakistan

[3] Physics Division, Directorate of Science, PINSTECH, Nilore, Islamabad, Pakistan

[4] Central Analytical Facility Division, Directorate of System and Services, PINSTECH, Nilore, Islamabad, Pakistan

(Received March 16, 2011 and accepted in revised form May 16, 2011)

Homogeneous crystalline 11mol.%magnesia doped partially stabilized zirconia (Mg-PSZ) and ZrO_2 ceramics with and without addition of sintering promoter oxides such as CuO, MnO_2 and CuO-MnO_2 were synthesized by hydrothermal treatment of zirconium and magnesium salts using sol spray process. The spray dried ZrO_2 and Mg-PSZ powders were calcined at 900°C and sintered upto 1200°C for 4 h. The relative density (~93% of theoretical) was achieved at 1100°C. The impact of sintering promoter oxides like 0.5mol % CuO, 0.5mol%MnO_2 and 0.5mol%CuO-MnO_2 on phase, microstructure development, texture properties (porosity, surface area, particle size distribution) and on the densification behavior of dense Mg-PSZ ceramic were examined. Sinterability of Mg-PSZ ceramic powder was found to depend upon the stoichiometric concentration of mixed salt solutions, flow rate of carrier gas and sintering promoter oxides. It was observed that both the Cu and Mn oxides are very effective as sintering aids. The small addition of sintering aid oxides, 0.5mol%CuO and 0.5mol%MnO_2 reduced sintering temperature (by ≈150-200°C) and promoted densification rate of Mg-PSZ with respect to the mixed CuO-MnO_2 addition. Addition of CuO enhanced the relative density and MnO_2 decreased the relative densities. However, the addition of mixed CuO-MnO_2 has an insignificant effect on the sintered density. The cubic structure $Mg_{0.2}Zr_{0.8}O_{1.8}$ was detected by X-ray diffraction. The scanning electron microscope analysis revealed that sintering aid oxides CuO and MnO_2 distorted surface morphology of Mg-PSZ nanocrystals rounded into dumb-belled shape with diameter of > 500nm.

Keywords: Sol sprays pyrolysis, Zirconia, Magnesia-doped zirconia, TG/DTA, Dilatometry, SEM, FTIR.

1. Introduction

Zirconia (ZrO_2) is a white crystalline insoluble ceramic oxide. It is superior in strength, toughness, ion conductivity, and chemical durability, and it is one of the essential oxides, which have attracted attention as raw materials for ceramics. Zirconia in its pure form is chemically inert but is a poor ceramic because of a mechanically damaging phase transformation that occurs in its crystal structure when it is cooled after firing. The polymorphic stability of zirconia over a broad temperature range is very important. Zirconia shows three polymorph phases with increasing temperature as given in equation 1 [1-2].

$$\text{Monoclinic} \xrightarrow{300-1000\,^{o}C} \text{Tetragonal} \xrightarrow{2370\,^{o}C} \text{Cubic} \xrightarrow{\text{above } 2370\,^{o}C} \text{Liquid} \quad (1)$$

At lower temperature, this phase transformation is accompanied by an expansion in volume of 3-4%. The change in volume associated with this transformation makes the usage of pure zirconia in many applications impossible. Addition of oxides 8mol% (3.81wt%) CaO, 8mol% (2.77wt %) MgO, or 3-4mol% (5.4-7.1wt %) Y_2O_3 into zirconia structure in a certain degree results a solid solution. This solid solution material is termed as partially stabilized zirconia (PSZ). While the addition of more than 16mol% of CaO (7.9wt %), 16mol% MgO (5.86wt %), or 8mol% of Y_2O_3 (13.75 wt %) into zirconia structure forms fully stabilized zirconia (FSZ). Its structure becomes cubic solid solution,

* Corresponding author : durranisk@gmail.com

which has no phase transformation from room temperature upto 2500^{o}C. The calcia, magnesia and yttria-doped partially stabilized zirconia (Ca-PSZ, Mg-PSZ and Y-PSZ) have been widely used in high-technology electronic and ceramic industries, particularly in wear parts and as solid electrolyte membrane in electrochemical devices due to their superior properties like mechanical strength, chemical durability and good ionic conductivity [3-5]. Since zirconia has a high melting point ~2680^{o}C temperatures in excess of 1600^{o}C are generally required for traditional fabrication techniques. The sintering promoters or aid oxide materials such as Al_2O_3, CuO, MnO_2 and SiO_2 have special characteristics and effectively used to modify the sintering rate and the mechanical properties i.e. hardness and toughness of the zirconia ceramic materials. Addition of these materials in different concentrations can effect on stability of tetragonal phase in tetragonal polycrystalline zirconia and also in doped-zirconia ceramic materials. However, in some cases, a negative effect on the conduction behaviour of stabilized zirconia has been observed [6]. The electronic and structural ceramic components require good homogeneity both in composition and microstructure, high purity and reliability. To be realized the ceramics having the above properties, fine grained, aggregation-free and narrow size distribution powders are required. The traditional process of synthesis of partially stabilized zirconia (Ca-PSZ, Mg-PSZ and Y-PSZ) is a solid state reaction based on calcining the mixed oxide or carbonate powders [7]. However, the calcined powder usually consists of chemically inhomogeneous particles with large grain sizes. This makes it hard to be used as raw material for advanced electronic components. Therefore, other wet chemical processes including co-precipitation [8], sol-gel [9], auto-combustion [10], hydrothermal [11], spray drying [12] and sol spray pyrolysis process [13] have been reported. The sol spray is one of the most promising process for the preparation of fine ceramic powders from their solutions using ultrasonic mist generation. The present work was carried out to study simple and economical sol spray process for synthesis of zirconia and Mg-PSZ ceramics at low temperature with and without addition of sintering aid transition metal-oxides. This paper details the codoping of 11mol%Mg-PSZ ceramic with 0.5mol%CuO, 0.5mol%MnO_2 and 0.5mol%CuO-MnO_2 in an attempt to reduce the sintering temperature and morphology variations of synthesized ceramic powders.

2. Experimental

All reagents used were analytical reagent grade and used without further purification. Carbonate free double distilled water (DDW) was used for solution preparation. Denitration of zirconium nitrate was performed using amberliteLA-2. Zirconium nitrate was dissolved in DDW and this solution was precipitated with ammonia to hydrolyzed zircomium (pH=6.85) hydro-thermally in a Teflon lined stainless steel autoclave at 180-225^{o}C for 5 h to make zirconia sol. The sol. was washed with DDW and calculated amount of magnesium nitrate was added to the zirconia sol according to its volume in order to get 11mol% Mg-PSZ milky-white sol. The sol. was dehydrated directly into powder by spraying it into a preheated temperature-controlled long quartz tube (length=750mm and diameter=25mm) using ultrasonic mist generator and sol spray process as described elsewhere [9,12-13]. The powder was allowed to remain in hot column for 30 minutes. The synthesized products with and without sintering aid oxides were labeled as Mg-PSZ, MgPSZ-Cu, MgPSZ-Mn, and MgPSZ-CuMn. The powder was calcined at 900^{o}C for 4h. The calcined powders were mixed with 2wt% polyvinyl alcohol (PVA) as binder material. Green and sintered pellets were prepared using uni-axil hydraulic press of load capacity 14 ton/in^2 (1 ton/in^2 =15.444 MPa). The green pellets were sintered in tube furnace (static air) at 1000-1200^{o}C for 4h. The sintered specimens were furnace cooled. The synthesized, calcined and sintered pellet specimens were characterized using different techniques such as thermogravimetry (TG), differential thermal analysis (DTA) X-ray diffraction (XRD) and Scanning electron microscope (SEM). Phase analysis and crystal structure was determined by XRD on a DMAX-IIIC Rigaku diffractometer with CuK_α (λ = 1.5418 A°) radiation. The XRD data were recorded in 2θ range from 15^{o}< 2θ < 80° by step scanning 0.05^{o} increments and scanning rate of 5^{o}/min. Microstructural features of specimens were observed by SEM (LEO 440i). The sintered pellets of Mg-PSZ, MgPSZ-Cu, MgPSZ-Mn, and MgPSZ-CuMn for SEM observation were put onto clean and polished aluminum stud and coated via thin layer of gold sputtering. For measurement of weight loss, combined TG/DTA thermal analysis was performed using a Netzsch STA-409

thermoanalyzer. Shrinkage and coefficient of thermal expansion of powder compacts were measured on high temperature computer-controlled differential dilatometer (Netzsch, DIL, 409) with heating rate of 10°C/min upto 1100°C in static air. Al_2O_3 reference was used for isothermal dimension change. The porosity and surface area of specimens were measured using Hg-diffusion using Penetrometer 08-0709 and nitrogen adsorption Brunauer, Emmett and Teller (BET) method [14] using Quantasorb sorption system (Quantachrome, USA). The apparent densities of specimens were measured using Ultra Pycnometer 1000 (Quantachrome) and verified by Archimedes' buoyancy method. Particle size distribution of powder materials was measured by dynamic laser light scattering using laser particle size analyzer.

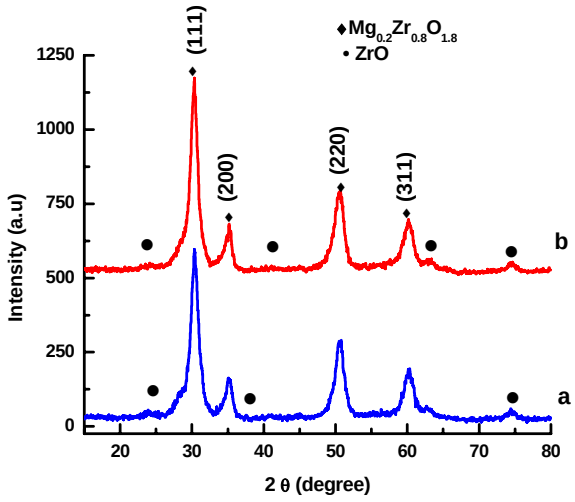

Figure 1. (a-b) XRD pattern of magnesia doped zirconia with and without sintering aids (a) Mg-PSZ (b) Mg-PSZ-Mn .

3. Results and Discussion

Figure 1 (a-b) shows the XRD pattern of synthesized and crushed sintered pellets of 11mol%magnesia doped zirconia and with addition of Mn-oxide. The pattern shows broad peaks indicate presence of nanosized crystals. Miller index were assigned according to JCPDS 75-0345 for $Mg_{0.2}Zr_{0.8}O_{1.8}$ (Fig.1a) and $Mg_{0.125}Mn_{0.125}Zr_{0.75}O_{1.8}$ (Fig.1b) respectively [15]. Three main peaks at (111), (200) and (220) of Mg-PSZ ($Mg_{0.2}Zr_{0.8}O_{1.8}$) were indicated monophase cubic structure with lattice parameters a = 5.08A^o and are consistent with reported values [16]. The sintering aid oxides (CuO and MnO_2) were found very effective in improving cubic phase content. It is noted that codoping of sintering aids (Cu^+ and Mn^{2+}) in Mg-PSZ was not distorted the cubic phase and the XRD peaks correspond to the Bragg angles for (111), (220) and (311) indicates the cubic phase of Mg-PSZ. The average crystallite size of Mg-PSZ was calculated about in range 67-100 A^o using Debye-Scherrr formula [17]. The average grain size increases with the increase of sintering temperature. When Mg-PSZ specimens were sintered at 1100°C for 4h with sintering aids, the grain size was found to be quite uniform. The XRD results demonstrate that the as-synthesized products are pure phase of Mg-PSZ with and without sintering aids.

Figure 2 (a-d) shows SEM images of dried powder and sintered specimens of Mg-PSZ. The Fig. 2a indicates a typical low-magnification SEM image of micro spherical particles of as-synthesized Mg-PSZ. These micros spherical have diameters in the range of (1.0-1.2μm). Some of them aggregate together and agglomerated, slightly porous and highly dispersed. The particle size distribution seems to be uniform. When aqueous solutions of inorganic salts such as nitrates were used as starting materials, hollow or porous particles were formed. This is because the thermal decomposition begins first around the outer surface of the droplet and solid shells are firmly produced during the very short period of reaction. Quite different morphology of crystals of sintered pellets Mg-PSZ (Fig.2b), Mg-PSZ-Cu (Fig.2c) and Mg-PSZ-Mn (Fig.4) was observed as compared to as-synthesized Mg-PSZ. The morphology of sintered Mg-PSZ crystals is slightly dumb-bell with non-uniform size distribution (Fig. 2b). The shape of crystals of Mg-PSZ-Cu and Mg-PSZ-Mn are found to be spherical to some extent but different than dumb-bell morphology (Fig. 2c and d). It is clear that sintering aid oxides (CuO and MnO_2) have affected morphology. Figure 2b revealed that in the sintered specimen of Mg-PSZ had mean grain size of about 2μm whereas a much higher grain size 3.5-4.2μm was observed from the sintered pellets of Mg-PSZ-Cu (Fig.2c) and Mg-PSZ-Mn (Fig.2d). It is observed that sintering aids CuO and MnO_2 have shown to be good additives for sintering of Mg-PSZ. The SEM analysis showed that nanocrystals with different morphologies and dimensions could be synthesized easily by sol spray process by changing the synthesis conditions and flow rate of

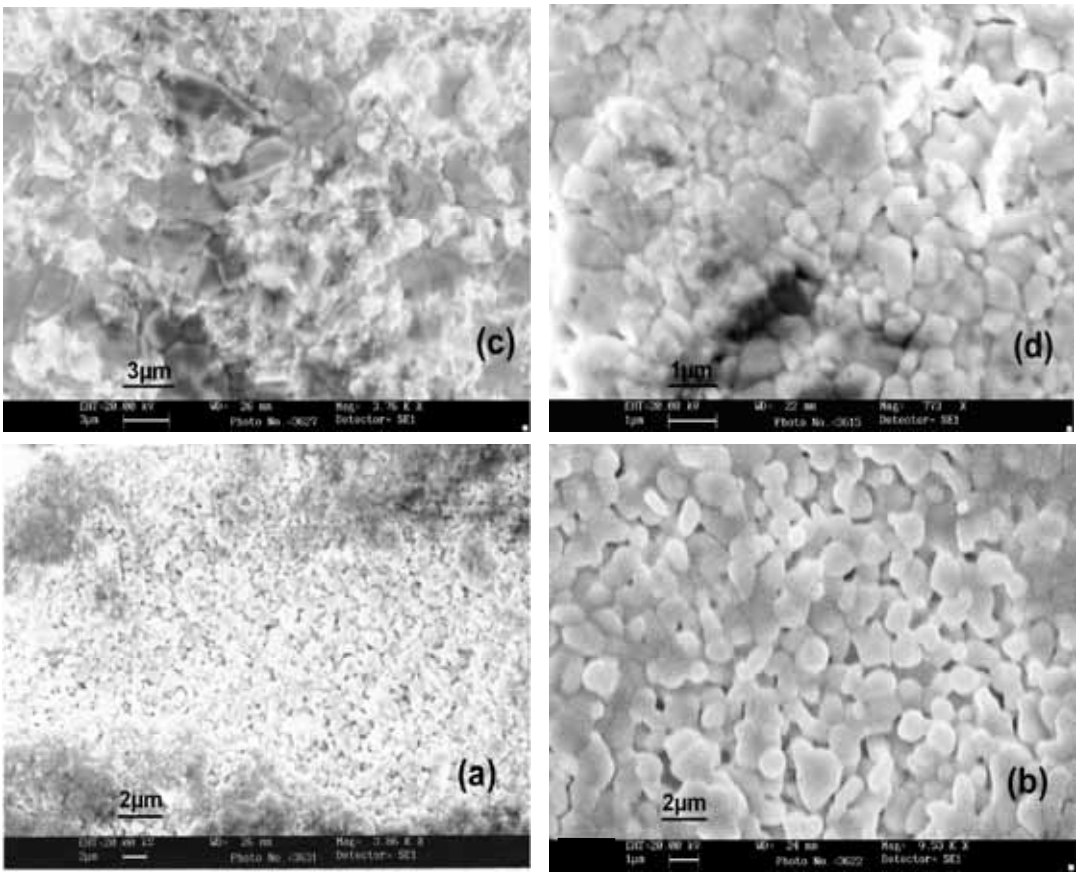

Figure 2 (a-d). SEM images of powder and sintered specimens of (a) As-synthesized Mg-PSZ powder (b) Mg-PSZ sintered pellet (c) Mg-PSZ-Cu sintered pettet and (d) Mg-PSZ-Mn sintered pellet.

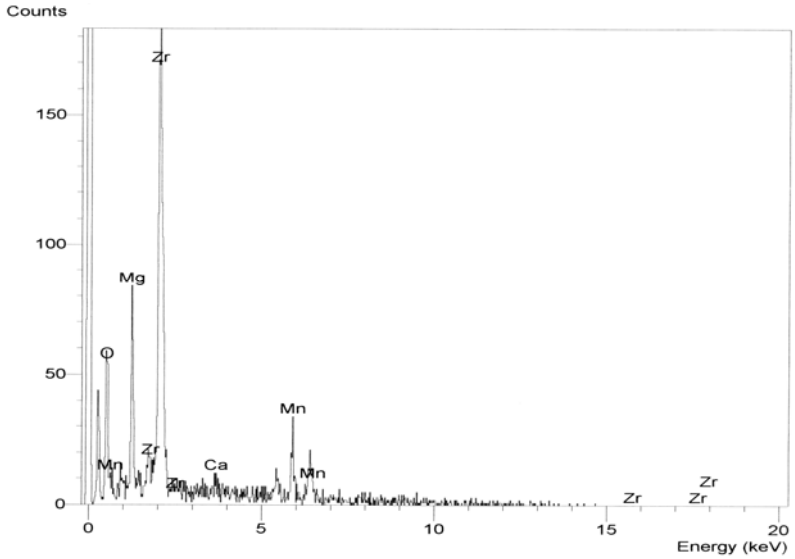

Figure 3. SEM (EPMA) spectrum of Mg-PSZ-Mn.

mist. Figure 3 shows the composition analysis of Mg-PSZ-Mn sintered at 1200^{o}C for 4 h estimated by electron probe micro analyzer (EPMA) attached with SEM. The chemical compositions of synthesized and sintered products were also measured by ICP and the analyzed results were

Table 1. Chemical composition and thermal analysis of zirconia and 11mol% magnesia doped partially stabilized zirconia with and without sintering aid oxides.

Specimens	Compositions (%)					Thermal analysis
	Zn	Mg	Cu	Mn	Oxygen + impurities	Weight loss (%)
ZrO_2	72.39 ± 0.4	ND	ND	ND	27.61 ± 0.2	11.57
Mg-PSZ	70.15 ± 0.2	2.28 ± 0.3	ND	ND	27.57 ± 0.3	7.73
Mg-PSZ -Cu	69.85 ± 0. 1	2.15 ± 0.2	0.66 ± 0.02	ND	27.34 ± 0.3	4.66
Mg-PSZ -Mn	71.25 ± 0.4	2.25 ± 0.1	ND	0.72 ± 0.05	25.78 ± 0.1	4.34
Mg-PSZ-CuMn	71.68 ± 0.5	2.19 ± 0.4	0.42 ± 0.05	0.68 ± 0.05	25.03 ± 0.2	4.55

Oxygen + impurities (by difference) Ca, Hf, Fe, K, Pb are major impurities.
ND = Not Detected.

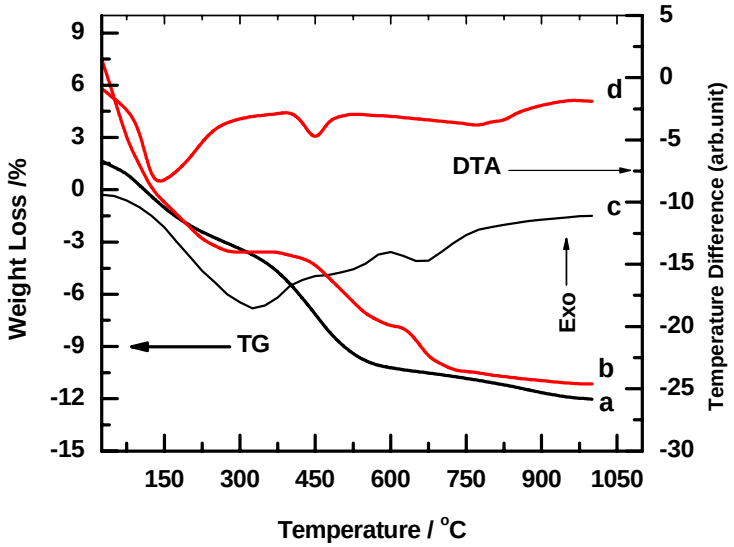

Figure 4 (a-d). Thermogravimetric (TG) and differential thermal analysis (DTA) traces of (a and c) ZrO_2 and (b and d) 11mol%Mg-PSZ ceramic powder synthesized by spray pyrolysis process.

found to be stoichiometrically uniform (Table 1). The unit cell formula was estimated using oxide formulae method [18].

Figure 4(a-d) shows the TG-DTA thermograms of as-synthesized dried ZrO_2 and Mg-PSZ ceramic powders derived from sol spray process. Endothermic and exothermic peaks were found with an overall weight of 11.57% and 7.73% for ZrO_2 and Mg-PSZ respectively and weight loss (%) values were summarized in Table 1. The decomposition reaction was endothermic; the endothermic DTA peak, Fig.4c around 120-370°C (max.323°C) is attributed to the dehydration of trapped water and decomposition of partial alkaline solution in dried ZrO_2 powder. Between 200 and 450°C, complexes formed by nitrate salts in solution and decomposed to form amorphous ZrO_2. However, the corresponding DTA curve Fig.4c shows an exothermic peak around at ~594°C.This indicates that there is no significant crystallization prior to that at ~600°C. The two endothermic

peaks, Fig.4d around 75-225°C (max.141°C) and 345-480°C (max.445°C) are due to evaporation of water absorbed and decomposition of un-reacted salts (nitrates) in Mg-PSZ. No exothermic peaks as well as other thermal effects were observed above 800°C in DTA curves Fig. 4d. All the volatiles were completely removed upto 900°C. The TG/DTA results were found to be comparable with the findings of Shane et al.[19].

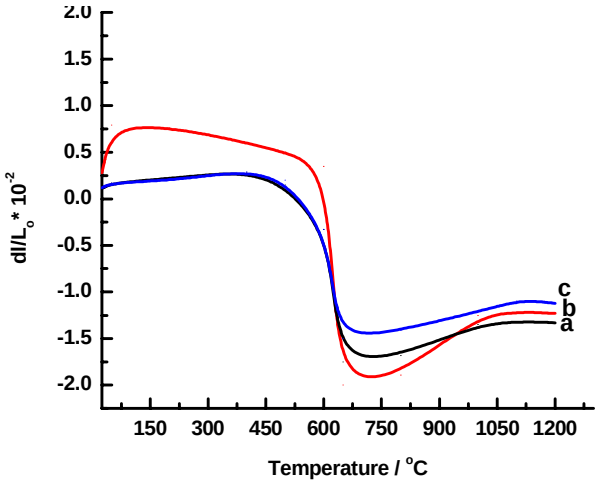

Figure 5 (a-c). Dilatometric spectra of 11mol% magnesia doped partially stabilized zirconia specimens with and without sintering aids (a) Mg-PSZ, (b) Mg-PSZ-Cu (c) Mg-PSZ-Mn

The behavior of pressed powders during sintering was examined by means of dilatometry. Figure 5 (a-c) shows dilatometry curves for three selected green pellets of Mg-PSZ, Mg-PSZ-Cu, and Mg-PSZ-Mn. The onset shrinkage temperature 450-600 °C remain unchanged by the addition of CuO and MnO_2 but powder behave differently after the initial shrinkage stage; the curves show a single-step densification and change in length during sintering of pressed pellets. There was no change in length on heating up to 290°C but started at about 570°C. The curves in Fig. 5(a,c) shrinkage started at 430°C. However, a large shrinkage occurred as a result of evolution of decomposed species between 420-635°C. The temperatures between 760-1050°C shows the expansion in material and these expansions are due to the decomposition/expulsion of organic binder (PVA). Above 650°C there is gradual increase in dimensional changes (lattice parameters) which are due to development of Mg-PSZ phase. On the basis of dilatometry results, sintering was conducted between 800-1000°C in order to obtain the full crystalline Mg-PSZ phase. Thermal expansion co-efficient (α) of Mg-PSZ, Mg-PSZ-Cu, and Mg-PSZ-Mn ceramic specimens measured at different temperature range 25-1150°C by diliatmetry and results are summarized in Table 2. The thermal expansion co-efficient of specimens Mg-PSZ-Cu, Mg-PSZ-Mn and Mg-PSZ-CuMn were found to be higher than Mg-PSZ. It is observed that sintering aid oxides enhanced thermal expansion co-efficient. The pressed specimen of zirconia (ZrO_2) show less thermal expansion co-efficient (α = 6.5 x10^{-6} °C^{-1}) as compared to magnesia doped zirconia with and without sintering aid oxides in temperature range of 30-1100°C. The results can be discussed in term of the level of agglomeration of the initial powder compacts and pinning of grain boundaries by the particles. Pure ZrO_2 is monoclinic at all temperatures; the nanocrystalline material exhibits a transformation from monoclinic to the tetragonal phase with maximum volume fraction of ~80% at 1050°C [20].

Densities of compact ceramic powders of Mg-PSZ with or without sintering aid oxides were estimated by Archimedes method and also using the equation as mentioned in [21] and the results are presented in Table 3.

$$\frac{\rho}{\rho_{th}} = \frac{\rho_o}{\rho_{th}} \left[1 - \frac{\Delta L}{L_o} \right]^{-3} \qquad (2)$$

Where ρ_o/ρ_{th} was the initial density, $\Delta L/L_o$ was the total relatively shrinkage measured from the dilatometry sintering studies, and ρ/ρ_{th} was the relative density of the sintered compact. Figure 6 (a-c) shows % relative densities of sintered compact Mg-PSZ with and without sintering aids as a function of sintering temperatures. It can be seen from Fig.6c that a sharp and regular increase densification is established between 900 and 1250°C reaching in most cases a maximum after which a less flat plateau is maintained at 1300°C. There is no further increase in densification after the density reached 93% of theoretical. The 93% relative density is achieved by Mg-PSZ at 1200°C.

The results revealed that sintered Mg-PSZ specimen is composed of uniformly sized grains and is >93% of theoretical density (relative density) comparable with the results of densities of powder compacts with work of Abraham and co-workers [8]. It was observed that addition of sintering aids

Table 2. Measurement of thermal expansion co-efficient .

Specimens	Length, L_o (mm)	Thermal expansion Co-efficient , α ($^oC^{-1}$)			
		ΔT (^oC)	α ($^oC)^{-1}$	ΔT (^oC)	α ($^oC)^{-1}$
ZrO_2	14.4	30-658	4.63×10^{-6}	30-1000	6.5×10^{-6}
Mg-PSZ	16.5	30-689	3.10×10^{-5}	30-1000	8.1×10^{-6}
Mg-PSZ -Cu	22.3	30-711	4.13×10^{-5}	30-1100	8.3×10^{-6}
Mg-PSZ -Mn	21.8	30-681	4.84×10^{-5}	30-1160	8.6×10^{-6}
Mg-PSZ-CuMn	25.8	30-781	5.31×10^{-5}	30-1150	8.8×10^{-6}

Table 3. Physico-chemical characteristics of zirconia and Mg-PSZ nanocrystalline ceramic.

Physico-chemical measurements	Specimens			
	Mg-PSZ	Mg-PSZ -Cu	Mg-PSZ -Mn	Mg-PSZ-CuMn
Green density (gm. cm^{-3})	2.62	1.51	1.79	2.48
Sintered density (gm.cm^{-3})	5.01	5.11	5.04	5.09
Relative density (%)	93.1	94.5	92.3	89.5
Crystalline size (nm)	34	36	29	39
Median diameter (μ m)	2.1	1.8	2.5	2.8
BET Surface area ($m^2.g^{-1}$)	46.7	44.3	53.4	56.5
BET crystalline size (nm)	26	27	23	21
Agglomeration coefficient (C)*	0.76	0.74	0.80	0.54

Density of plane ZrO_2 = 4.5 g.cm^{-3} *$C = d_{BET}/D$.

oxide (CuO- MnO_2) in Mg-PSZ decrease the sintering temperature and suppressed abnormal nucleation and growth. As a result, the densification rate increased and a uniform structure was obtained. The Cu and Mn oxides were found to decrease more than 100^{o}C sintering temperature of Mg-PSZ with respect of mixed CuO-MnO_2 addition. It was observed that sintering aids restrained the grain growth of Mg-PSZ ceramic materials. Addition of CuO enhanced the relative density Fig.6c while MnO_2 decreased the relative densities Fig.6a.

Figure 7(a-d) illustrates the particle size distribution of ZrO_2 and Mg-PSZ ceramic powders. The particle size distribution curves revealed that the median diameter of Mg-PSZ was 3.6 micron and that of fine ZrO_2 particle was 1.2 micron. It means that the particles produced by sol spray method tend to be somewhat hollow spherical with more porosity. The median diameter of particles of Mg-PSZ with and without sintering aid ceramic powders is presented in Table 3. It is anticipated that ceramic materials undergo changes in phase transformation as the particle size distribution is twisted. When synthesized material grows in micron size or as the grain size is reduced, the surface area grows in comparison with volume and it becomes enhance.

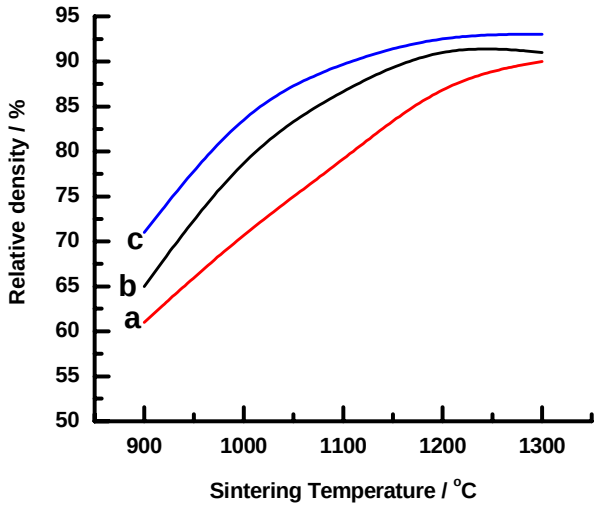

Figure 6 (a-c). Percent relative densities as a function of sintering of magnesia doped zirconia with and without sintering aids (a) Mg-PSZ (b) Mg-PSZ-Cu (c) Mg-PSZ-Mn.

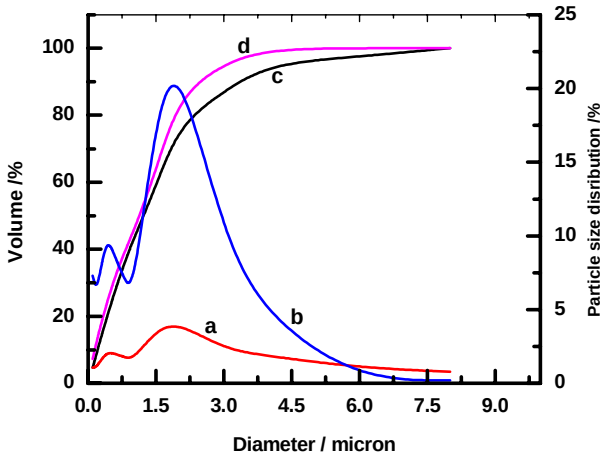

Figure 7 (a-d). Particle size distribution of ZrO_2 and 11mol% Mg-PSZ ceramic powder materials. (a and c) ZrO_2 (b and d) 11mol% Mg-PSZ.

The BET surface area of Mg-PSZ with and without sintering aids were found in range of 44.3 - 56.5 $m^2.g^{-1}$ respectively and the results were found consistent with literature [22]. It can be seen that the surface area and particle size distribution values were altered with the addition of sintering aid oxides in Mg-PSZ. The specific surface area were estimated by BET method at liquid nitrogen temperature and mean grain size (crystallite size) can be figured out according to Chen et al.[23] assuming that powders are constituted of non-porous spherical particles. The comparison of the geometric surface, calculated either from the mean diameter of crystallites obtained by broad peaks of XRD pattern with the specific surface area measured by BET gives indications on the porosity or the nature of elementary grains mono or polycrystalline. The size determined by XRD was normally regarded as the size of the primary crystallites (denoted D), and the size deduced from the BET method (d_{BET}) can be used as the size of the mean agglomerated particles and the ratio is regarded as the mean agglomerated coefficient of the nanocrystals powders. The agglomeration coefficient was calculated using Chen et al. [23] formula. The agglomeration coefficient Mg-PSZ was found ~1.84 which indicates that the agglomeration was more evident in nanosized Mg-PSZ powder, Table 3.

4. Conclusion

Pure white 11mol. %Mg-PSZ ceramic powders with and without addition of sintering aid oxides (CuO, MnO_2 and CuO-MnO_2) have been synthesized by sol spray pyrolysis from nitrate salt solutions using an ultrasonic mist generator. The dumb bell spherical particles of Mg-PSZ was obtained with median particle median diameter (~1.1µm). The particle characteristics were affected by stoichiometric concentration of salt solutions and the flow rate of carrier gas. When the concentration increased, particles in diameters of ~0.6 to 0.8µm were appeared; however the low flow rate of carrier gas can generate the more fine particles. The prepared ceramic powders showed excellent compaction characteristics (93% dense Mg-PSZ) ceramics at sintering temperatures 1100°C. Additions of CuO enhance %relative density while the presence of MnO_2 and both CuO-MnO_2 decrease the %relative densities. The median particle diameter (µm) and BET surface area were decreased by addition of CuO while MnO_2 and both CuO-MnO_2 enhance the median diameter and BET surface area. It is also observed that addition of crystal growth inhibitor CuO and MnO_2 lowers the sintering temperature and suppresses abnormal nucleation and growth. As a result, the densification rate was increased and a uniform structure was obtained.

References

[1] H. Boysen, F. Frey and T. Vogt, Acta, Cryst., **B46** (1990) 724.

[2] J. M. Leger, P.E. Tomaszewski, A. Atouf and A.S. Pereira, Phy. Rev. **B47** (1993) 14075.

[3] F.T.C Lacchi, K. M. Crane and S.P.S. Badwal, Solid State Ionics **73** (1994)49.

[4] M.A.C.G. Van De Graaf and A.J. Burggraaf, in Advances in Ceramics, Vol. 12, Science and Technology of Zirconia II, A.H. Heuer and L.W. Hobbs (Ed.), American Ceramic Society, OH, (1984).

[5] S. Chen, W. Deng and P. Chen, Mater. Sci. Eng. **B22** (1994) 247.

[6] K. Keizer, A.J. Burggaaf and G.DE With, J. Mater. Sci. **17** (1982)1095.

[7] S. K. Durrani, J. Akhtar, M. A. Hussain, M. Arif and M. Ahmad, Mat. Chem. Phys. **100** (2006) 324.

[8] I. Abraham and G. Gritzner, J. Mater. Sci. Lett. **12** (1993) 995.

[9] J. Akhtar, S. K. Durrani, N. A. Chughtai and K. A. Shahid, J. Chem. Soc. Pak. **19** (1997) 93.

[10] T. Mimani and K.C. Patil, Mater. Phys. Mech., **4**1 (2001) 1.

[11] S. Somiya and R.Roy , Butt. Mater. Sci. **23** (2000) 435.

[12] S. K. Durrani, A. H. Qureshi, S. Qayyum and M. Arif. J. Therm. Anal. Calori. **95** (2009) 87.

[13] S. K. Durrani, K.Saeed, A. H. Qureshi, M. Ahmad, M. Arif, N.Hussain and T. Mohammad, J. Therm. Anal. Calori. **104** (2011) 645.

[14] S. Brunauer, P.H. Emmett and E. Teller, J. Amer. Chem. Soc. **60** (1938) 309.

[15] H. Ishizawa, O. Sakural, N. Mizutani and M. Kato, Yogyo-Kyokaishi **93** (1985) 382.

[16] International Centre for Diffraction Data, JCPDS Card, (2002).

[17] B. D. Culity, S. R. Stock, Elements of X-Ray Diffraction, Addition-Wesley, MA, (1978).

[18] D. M. Roy, R.R. Neugaonka, T.P. Holleran, and R. Roy, Am. Ceram. Soc. Bull. **56** (1977) 1023.

[19] M. Shane and M. L. Macartney, J. Mater. Sci. **25** (1990) 1537.

[20] G. Scipione, Mat. Sci. Forum. **269-272** (1998)207-212.

[21] B. Fegley, Jr., P. White and K. H. Bowen, Am. Ceram. Soc. Bull. **66** (1987)1342.

[22] K. C. Bradford and R. J. Bratton, J. Mater. Sci. **14** (1979) 59.

[23] C. C. Chen, P. Liu and C. Lu, Chem. Eng. J. **144 (**2008) 509.